Incident Power Density Assessment Study for 5G Millimeter-Wave Handset Based on Equivalent Currents Method

He, Wang; Scialacqua, Lucia; Scannavini, Alessandro; Ying, Zhinong; Zhao, Kun; Xu, Bo; Paola, Carla di; Zhang, Shuai; He, Sailing

Published in:
2020 14th European Conference on Antennas and Propagation (EuCAP)

DOI (link to publication from Publisher):
10.23919/EuCAP48036.2020.9135622

Creative Commons License
Unspecified

Publication date:
2020

Document Version
Accepted author manuscript, peer reviewed version

Link to publication from Aalborg University

Citation for published version (APA):
He, W., Scialacqua, L., Scannavini, A., Ying, Z., Zhao, K., Xu, B., Paola, C. D., Zhang, S., & He, S. (2020). Incident Power Density Assessment Study for 5G Millimeter-Wave Handset Based on Equivalent Currents Method. In *2020 14th European Conference on Antennas and Propagation (EuCAP)* [9135622] IEEE. Porceedings of the IEEE European Conference on Antennas and Propagation (EuCAP) https://doi.org/10.23919/EuCAP48036.2020.9135622

Incident Power Density Assessment Study for 5G Millimeter-Wave Handset Based on Equivalent Currents Method

Wang He[1], Lucia Scialacqua[2], Alessandro Scannavini[2], Zhinong Ying[3], Kun Zhao[3, 5],
Bo Xu[4], Carla Di Paola[5], Shuai Zhang[5], Sailing He[1]
[1] Centre for Optical and Electromagnetic Research, Zhejiang University, Hangzhou, China, whe@zju.edu.cn
[2] Microwave Vision Italy, Pomezia, Italy
[3] Sony Research Center, Sony Corp., Lund, Sweden
[4] Ericsson Research, Ericsson AB, Stockholm, Sweden
[5] Antenna, Propagation and mm-Wave Systems Section, Department of Electronic Systems, Aalborg University, Denmark

***Abstract*—When placed on the market, mobile handsets are required to comply with relevant electromagnetic field (EMF) exposure limits. In the millimeter-wave (mmWave) frequency band, human exposure to EMF needs to be evaluated in terms of incident power density (PD). In this work, the equivalent currents (EQC) method is applied to assess the PD of a 5G mmWave mobile handset mock-up. The PDs in the near field (NF) region are obtained using the field data measured in the intermediate field (IF) region with an MVG mmWave spherical measurement system. The results are compared with those obtained by simulations and also with those obtained by reference NF scanning measurements. The agreement between the methods indicates that the EQC method is a promising candidate for the PD assessment of 5G mmWave handsets.**

***Index Terms*—5G, incident power density, field reconstruction, mobile handset, millimeter wave.**

I. INTRODUCTION

The fifth generation (5G) mobile communication system has been rolled out in some countries since 2018. In the millimeter-wave (mmWave) frequency band, much larger bandwidth is available for 5G compared to the bands below 6 GHz. According to the technical specification released by the 3rd Generation Partnership Project (3GPP) [1], the operating bands of 5G New Radio (NR) in the mmWave frequencies include those from 24.25 GHz to 29.5 GHz and from 37 GHz to 40 GHz. Above 6 GHz, the incident power density (PD) of the equipment under test (EUT) shall be used to evaluate human exposure to electromagnetic fields (EMFs), and in addition, the PD above 30 GHz shall be spatially averaged over an area of 1 cm^2, according to the draft EMF guidelines by the International Commission on Non-Ionizing Radiation Protection (ICNIRP) [2].

For a 5G mobile handset working in close proximity to the human body, PD needs to be evaluated at close distances to the handset within the near field (NF) of the equipped antennas. The direct measurements in the NF will cause mutual coupling between the antenna(s) and the probe, thus probe compensation [3], [4] is required. Besides, for traditional NF scanning measurements, the planar or volumetric scanning is time-consuming. Recently, research done by Sasaki *et al.* applies the plane-wave spectrum expansion technique for PD assessment in the mmWave band [5], in which the NF strength is reconstructed from the measured field strength in the intermediate field (IF) or the far field (FF). However, the plane-wave expansion technique usually transforms the EMFs in the range between the measurement plane and the EUT, so it can only reconstruct the PD on one side of the EUT at a time. For the EUT without the prior knowledge about the maximum PD directions, the same measurement procedure may need to be repeated several times in different directions.

In this work, the equivalent currents (EQC) method is investigated for the PD assessment of a 5G mmWave mobile handset mock-up. Compared to the plane-wave expansion technique, the PD distribution of the handset in all directions can be reconstructed by the EQC method in one measurement. The EQC method is based on dual-equation formulation [6]–[8]: one equation constraints that the EQC radiates the measured field, and the other equation enforces the Love's equivalence form. By such method, the electric and magnetic EQC over a reconstruction surface enclosing the EUT can be reconstructed using the IF or FF data. Then, the reconstructed EQC can be used to calculate the field strength outside the reconstruction surface. A 5G handset mock-up equipped with four quasi-Yagi antennas is employed in this research. The PD at 38 GHz in the NF region is reconstructed by the EQC method and compared with the results from simulation and the reference measurements.

II. METHOD AND MODEL

A. Equivalent Currents Method

The EQC method in this work constraints that the EQCs, i.e. $\mathbf{J}_{\mathrm{eq}}$ and $\mathbf{M}_{\mathrm{eq}}$, over the reconstruction surface, Σ_{R}, radiates the measured IF or FF strength over the measurement surface, Σ_{M} [6]–[8]:

$$\hat{\mathbf{n}} \times \mathbf{E}(\mathbf{r}) = \hat{\mathbf{n}} \times \left[-\eta_0 \mathcal{L}(\mathbf{J}_{\mathrm{eq}};\mathbf{r}) + \mathcal{K}(\mathbf{M}_{\mathrm{eq}};\mathbf{r})\right] \quad \mathbf{r} \in \Sigma_{\mathrm{M}} \quad (1)$$

where

$$\mathcal{L}(\mathbf{J}_{\mathrm{eq}};\mathbf{r}) = jk_0\int_{\Sigma_{\mathrm{R}}}\left[\mathbf{J}_{\mathrm{eq}}(\mathbf{r}')+\frac{1}{k_0^2}\nabla\nabla'_s\cdot\mathbf{J}_{\mathrm{eq}}(\mathbf{r}')\right]g(\mathbf{r},\mathbf{r}')\mathrm{d}s' \tag{2a}$$

$$\mathcal{K}(\mathbf{M}_{\mathrm{eq}};\mathbf{r}) = \int_{\Sigma_{\mathrm{R}}}\mathbf{M}_{\mathrm{eq}}(\mathbf{r}')\times\nabla g(\mathbf{r},\mathbf{r}')\mathrm{d}s' \tag{2b}$$

$$g(\mathbf{r},\mathbf{r}') = \frac{e^{-jk_0|\mathbf{r}-\mathbf{r}'|}}{4\pi|\mathbf{r}-\mathbf{r}'|} \tag{2c}$$

where $\eta_0=\sqrt{\mu_0/\epsilon_0}$, $k_0=\omega\sqrt{\mu_0\epsilon_0}$, and ∇'_s is the surface divergence operator. Equation (1) is established by making the radiated field of $\mathbf{J}_{\mathrm{eq}}$ and $\mathbf{M}_{\mathrm{eq}}$ have the same tangential component with the measured IF or FF over Σ_{M}.

Boundary integral identities are also used to enforce Love's form for EQCs:

$$\hat{\mathbf{n}}\times\left[-\eta_0\mathcal{L}(\mathbf{J}_{\mathrm{eq}};\mathbf{r})+\mathcal{K}(\mathbf{M}_{\mathrm{eq}};\mathbf{r})\right] = -\frac{1}{2}\mathbf{M}_{\mathrm{eq}}(\mathbf{r})\ \mathbf{r}\in\Sigma_{\mathrm{R}} \tag{3a}$$

$$\hat{\mathbf{n}}\times\left[-\frac{1}{\eta_0}\mathcal{L}(\mathbf{M}_{\mathrm{eq}};\mathbf{r})-\mathcal{K}(\mathbf{J}_{\mathrm{eq}};\mathbf{r})\right] = \frac{1}{2}\mathbf{J}_{\mathrm{eq}}(\mathbf{r})\quad \mathbf{r}\in\Sigma_{\mathrm{R}} \tag{3b}$$

The EQC reconstruction calculation based on the above formulations is implemented in the software INSIGHT provided by Microwave Vision Group (MVG) [9]. After reconstruction, the EQCs are imported into the commercial software CST Studio Suite [10] to calculate the field strength outside Σ_{R}. The peak spatial-averaged PD (*psaPD*) can be calculated by [11], [12]:

$$psaPD^A(d) = \max_{all\ A\ at\ d}\left(\frac{1}{2A}\iint_A \mathrm{Re}[\mathbf{E}\times\mathbf{H}^*]\cdot\hat{n}\,\mathrm{d}A\right) \tag{4}$$

where A is the averaging area, i.e., 1 cm^2 in this work, d is the distance from EUT, $\hat{n}$ is the unit vector normal to A, and the superscript $*$ denotes the complex conjugate.

B. Handset Mock-up

Fig. 1 shows the handset mock-up used in this work [13]. The total size of the mock-up is $70\,\mathrm{mm}\times130\,\mathrm{mm}\times0.76\,\mathrm{mm}$. Four quasi-Yagi antennas are designed at the upper-right corner orienting to different directions, denoted as Ant 1 to Ant 4. They are excited at 38 GHz in this work, and the input power of each antenna is normalized to 5 dBm.

The IF of the mock-up is measured by StarLab 50 GHz [14], which collects the tangential component of electric field over a sphere, i.e., Σ_{M}, with radius of 450 mm, as shown in Fig. 2 (a). To perform EQC method, a reconstruction surface Σ_{R} is built enclosing the mock-up with 3 mm distance in $\pm x$- and $\pm y$-directions and 5 mm distance in $\pm z$-directions. The larger distance in $\pm z$-directions is considering the length of the connectors.

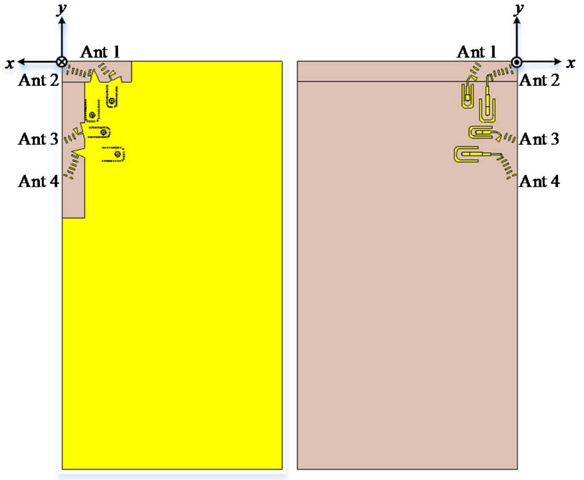

(a) (b)

Fig. 1. The (a) bottom and (b) top view of the handset mock-up.

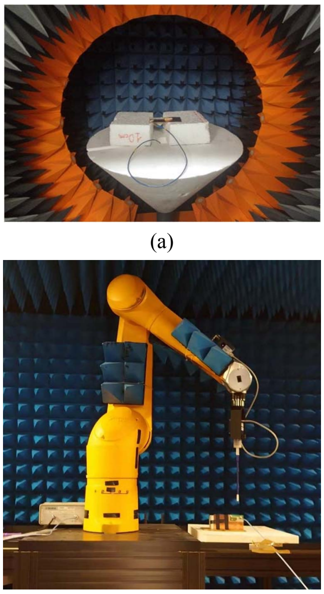

(a)

(b)

Fig. 2. (a) The IF measurement by StarLab 50 GHz and (b) the reference measurement using SPEAG cDASY6 mmWave Module V1.0 and EUmmWV3 probe.

C. Reference Measurement

As a comparison to the EQC method results, the reference measurements were conducted using SPEAG cDASY6 mmWave Module [15] V1.0 and EUmmWV3 probe [16], as shown in Fig. 2 (b). The electric and magnetic field strength were measured and the *psaPD* was calculated at distances of 5 mm, 10 mm, 15 mm, 20 mm, and 25 mm away from the edge of the mockup in the $+x$-direction for Ant 2 and Ant 3 at 38 GHz.

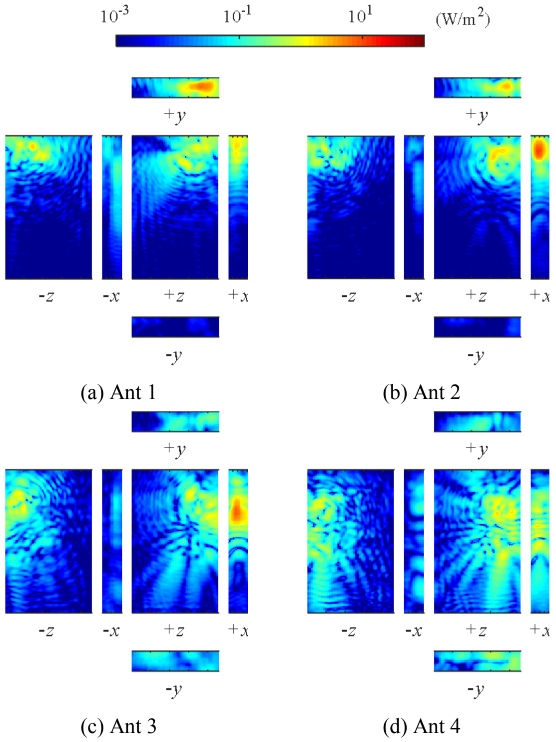

(a) Ant 1 (b) Ant 2

(c) Ant 3 (d) Ant 4

Fig. 3. The PD distributions in $\pm x$-, $\pm y$- and $\pm z$-directions for Ant 1–4 on a closed box surface embracing the mock-up with a 10 mm gap.

III. RESULT AND DISCUSSION

Here, using the measured IF data, the reconstructed PD distributions in $\pm x$-, $\pm y$- and $\pm z$-directions are presented for each antenna, as shown in Fig. 3. The distributions are on a closed box surface embracing the mock-up with a 10 mm gap. From these images, the direction and location of the maximum PD of each antenna can be easily found. For example, Ant 1 has strongest radiation towards $+y$-direction, while Ant 2 and Ant 3 radiate strongly in $+x$-direction. In practice, these images give an insight to observe the PD distribution and determine the direction and location of the maximum PD. Further measurements or evaluations could then be focused on that direction and location if necessary.

Fig. 4 shows the *psaPD* reconstructed by the EQC method versus the evaluation distance d. For comparison, the *psaPD* calculated in the full-wave simulation of the mock-up is also provided, as well as the results from the reference measurements. Considering the orientation of the quasi-Yagi antennas, only the *psaPD* in the direction of the maximum PD are presented, i.e., the $+y$-direction for Ant 1 and the $+x$-direction for Ant 2–4. Generally, the *psaPD* computed from the EQC method is close to that computed in the full-wave simulation. The largest difference between them appears at Ant 4. The difference might be attributed to the existence of cable and platform in the measurement. For Ant 2 and Ant 3, the *psaPD* results obtained from reference measurements agree well with the reconstructed and simulated results.

Fig. 5 shows the distributions of PD magnitude in the xy-plane in the NF region. The reconstructed distributions are similar to the corresponding simulation results. The blank in the reconstructed distribution suggests the space within Σ_R.

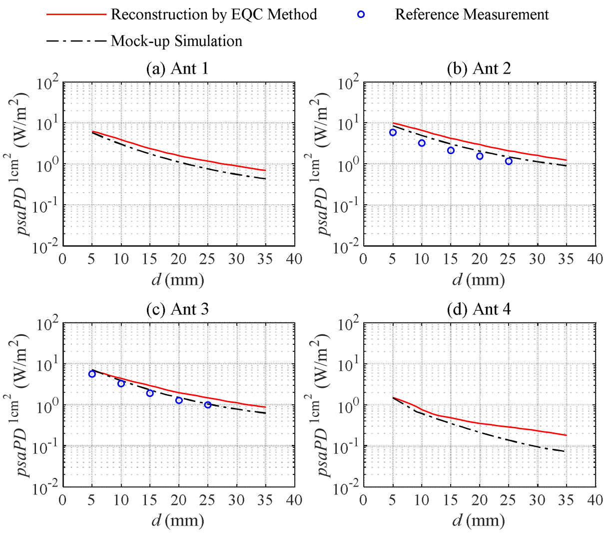

Fig. 4. The *psaPD* from the reconstruction, simulation and measurement versus the evaluation distance.

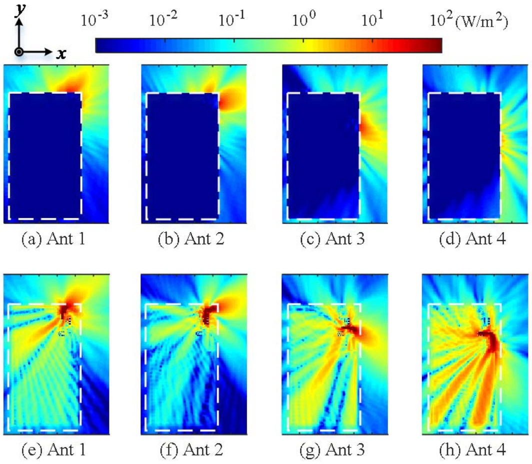

(a) Ant 1 (b) Ant 2 (c) Ant 3 (d) Ant 4

(e) Ant 1 (f) Ant 2 (g) Ant 3 (h) Ant 4

Fig. 5. The distributions of the PD magnitude in the xy-plane in the NF region. (a)–(d) are reconstructed and (e)–(h) are simulated.

Both Fig. 4 and Fig. 5 indicate that the EQC method using the IF measurement data is a promising candidate to assess the PD at close distances of 5G mmWave handsets.

IV. CONSLUSION

In this work, the equivalent currents (EQC) method with the spherical measurement system is applied to the incident power density (PD) assessment for a 5G handset at 38 GHz using the field strength obtained in the intermediate field (IF) region. The reconstructed PD distributions over a closed box surface provide an insight to determine where the maximum PD is. Good agreement between the reconstructed results, the simulated results, and the results obtained from the reference measurements can be observed. Therefore, the EQC method is a promising method for the PD assessment of 5G mmWave handsets.

REFERENCES

[1] *5G; NR; User Equipment (UE) radio transmission and reception; Part 2: Range 2 Standalone*, document TS 38.101-2, 3GPP, Rev. 15.3.0, Oct. 2018.

[2] *Draft Guidelines for Limiting Exposure to Time-Varying Electric, Magnetic and Electromagnetics Fields (100 kHz to 300 GHz)*, document, ICNIRP, Jul. 2018.

[3] D. Paris, W. Leach and E. Joy, "Basic theory of probe-compensated near-field measurements," *IEEE Trans. Antennas Propag.*, vol. 26, no. 3, pp. 373–379, May 1978.

[4] W. B. Joy, W. Leach, G. Rodrigue and D. Paris, "Applications of probe-compensated near-field measurements," *IEEE Trans. Antennas Propag.*, vol. 26, no. 3, pp. 379–389, May 1978.

[5] K. Sasaki, K. Li, J. Chakarothai, T. Iyama, T. Onishi and S. Watanabe, "Error analysis of a near-field reconstruction technique based on plane wave spectrum expansion for power density assessment above 6 GHz," *IEEE Access*, vol. 7, pp. 11591–11598, Feb. 2019.

[6] J. L. A. Quijano and G. Vecchi, "Improved-accuracy source reconstruction on arbitrary 3-D surfaces," *IEEE Antennas Wireless Propag. Lett.*, vol. 8, pp. 1046-1049, 2009.

[7] J. L. A. Quijano and G. Vecchi, "Field and source equivalence in source reconstruction on 3D surfaces," *Progress In Electromagnetics Research*, no. PIER 103, pp. 67–100, 2010.

[8] J. L. A. Quijano and G. Vecchi, "Near- and Very Near-Field Accuracy in 3-D Source Reconstruction," *IEEE Antennas Wireless Propag. Lett.*, vol.9, pp.634–637, 2010.

[9] Mivrowave Vision Group. *INSIGHT*. [Online]. Available: https://www.mvg-world.com/en/products/field_product_family/antenna-measurement-2/insight

[10] Computer Simulation Technology (CST). [Online]. Available: https://www.cst.com

[11] B. Xu, K. Zhao, Z. Ying, D. Sjöberg, W. He and S. He, "Analysis of impacts of expected RF EMF exposure restrictions on peak EIRP of 5G user equipment at 28 GHz and 39 GHz bands," *IEEE Access*, vol. 7, pp. 20996–21005, Feb. 2019.

[12] B. Xu, K. Zhao, B. Thors, D. Colombi, O. Lundberg, Z. Ying and S. He, "Power density measurements at 15 GHz for RF EMF compliance assessments of 5G user equipment," *IEEE Trans. Antennas Propag.*, vol. 65, no. 12, pp. 6584–6595, Dec. 2017.

[13] C. D. Paola, S. Zhang, K. Zhao, Z. Ying, T. Bolin and G. F. Pedersen, "Wideband beam-switchable 28 GHz quasi-yagi array for mobile devices," *IEEE Trans. Antennas Propag.*, accepted.

[14] Datasheet of StarLab 50 GHz. [Online]. Available: https://www.mvg-world.com/zh-hans/system/files/datasheet_starlab_5g_ch _03_18_bd.pdf

[15] cDASY6 Module mmWave, Schmid & Partner Engineering AG. [Online]. Available: https://speag.swiss/products/dasy6/software/5g-module-of-cdasy6/

[16] E-Field mm-Wave Probe for General Near-Field Measurements, Schmid & Partner Engineering AG. [Online]. Available: https://speag.swiss/products/dasy6/probes/new-eummwvx-vector-e-probe/